Moroccan Journal of Chemistry
ISSN: 2351-812X
http://revues.imist.ma/?journal=morjchem&page=login
Derouiche & al. / Mor. J. Chem. 9 N°4 (2021) 762-775
DOI: https://doi.org/10.48317/IMIST.PRSM/morjchem-v9i4.26108

Characterization and Corrosion resistance study of aeronautical aluminum 2024-T4 and 7075-T6 alloys

A. Derouiche[1], M. R. Kabiri[2], A. El Assyry[1*], M. Mourabit[1], K. Tariq[1]

[1]*Laboratory of Polymer Physics, Mechanical Sciences and Materials (LPPSMM), Faculty of Science Ben M'Sik, Hassan II University, Casablanca, Morocco.*
[2]*Laboratoire de Corrosion et Vieillissement, Département Matériaux et Procédés, ENSAM, Moulay Ismail University, Meknès, Morocco*

** Corresponding author:*
abdeslam_elassyry@yahoo.fr
Received 22 April 2021,
Revised O6 Dec 2021,
Accepted 06 Dec 2021

Abstract

Aluminum is one of the most used metals in the field of aeronautics, indeed, depending on the elements to which it is combined, it has interesting mechanical properties and corrosion resistance. The main objective of this work is to characterize the aluminum 2024 and 7075 alloys most used in the aeronautical field whose additive elements are respectively copper and zinc, to do this, we carry out heat treatment hardening structural to improve their mechanical properties such as corrosion resistance, and a range of tests to study their behavior in corrosive and oxidizing environments.

Keywords: *characterization, corrosion, aeronautical, aluminum, 2024-T4 alloys, 7075-T6 alloys*

1. Introduction

High-strength aluminum alloys occupy a prominent place in the field of aeronautical transport. Currently about 80% of the weight of the empty structure of a civil transport aircraft is made up of these Al alloys. This leading position has been maintained thanks to the improvements made to the alloys, and the development of grades with high mechanical strength, high toughness, and good corrosion resistance. However, the elements added to pure Al to improve their properties (Zn, Cu, Si, etc.), make it susceptible to corrosion. This corrosion can interact with mechanical stresses by stress corrosion and/or corrosion fatigue and lead to real lifetimes less than the estimated lifetimes. Corrosion action on crack type defects is therefore a danger to structures integrity. Among the most used alloys in Aeronautics, we find the 2000 series (Al-Cu) and the 7000 series (Al-Zn) [1, 2]. They have a low density which is an asset for reducing the airplanes mass. In addition, they have high mechanical characteristics which allows their use as structural materials. The mechanical resistance of these alloys is increased by the structural hardening phenomenon which involves specific thermal or thermomechanical treatments. The counterpart of these treatments is the establishment of a very heterogeneous microstructure which sensitizes the material to various modes of corrosion. As the pure metals, more than 99.5% of these materials have poor mechanical properties. This is the reason why, from the end of 19th century, metallurgists sought to improve several of its properties by adding other metals. In fact, we can consider that the metallurgy of Al really begins only with the discovery of the structural hardening of Al alloys to copper [3]. Al does not exist in its natural state, it was first produced by Deville [4]; It is a malleable metal of silver color, remarkable for its lightness (ρ= 2.7 g/cm^3) which is of great interest in the automotive and aeronautical industries, and more particularly in the design of aircraft. On the other hand, Al presents the most used metal after iron, its main mineral is bauxite, it is present in the form of hydrated oxide from which the alumina is extracted. It can also be extracted from nepheline from sillimanite leukitis, andalusite, and muscovite. However, the Al mechanical properties are poor, which limits the use of pure Al in industry [5]. The addition of other metals to form alloys considerably improves the mechanical properties and allows the use of these alloys as structural materials. However, these changes to the chemical composition are often made at the expense of their resistance to corrosion. It is therefore essential to adopt a compromise between the various properties sought [6-8, 9]. *2024 (Al-Cu) alloys*: contains a large amount of magnesium which improves structural hardening. It is therefore part of the sub-family of Al-Cu-Mg alloys. The other alloying elements (Mn, Fe and Si) allow the precipitation of quaternary compounds which improve the matrix properties. The chemical composition of 2024 alloy is presented in the following table:

Table.1. 2024 alloy chemical composition.

Element	Al	Cu	Mg	Mn	Fe	Si	Zn
% mass	>93	4.4	1.5	0.6	0.2	0.1	0.1

The Al-Cu system was one of the first to be industrially exploited under the name "duralumin" which was, for a long time, the commercial and usual name of Al alloys with 4% copper of the 2000 family; the addition of copper has several effects:

- Increase in the mechanical characteristics of Al, with a cap at around 6%. The increase in mechanical characteristics is due to the hardening phase Al_2Cu which precipitates during structural hardening [10].
- Reduce the folding ability of Al-Mg-Si alloys if the content exceeds 0.4% [11].
- It very clearly decreases the corrosion resistance because Cu weakens the natural oxide film properties [12]. In addition, the conditions of the structural hardening heat treatment are important parameters on which their sensitivity to corrosion depends, since they have an influence on the alloy corrosion potential [13].

- Greatly increases the sensitivity to hot cracking [14] to the point that Al-Cu alloys are not arc weldable, unless the Cu content reaches 6%, which is the case with 2219.

Physical and mechanical properties of the 2024 alloy are described elsewhere [15]: ρ= 2.77 g/cm^3, Melting interval= 500-638, Elasticity module= 73000 MPa, Thermal conductivity (0 at 100°C)= 120 W/M°C, Resistivity to 20°C= 5.7 µ'Ωcm, Elastic limit= 300 MPa, Limit at break R_m= 440 MPa, Mass thermal capacity (0 at 100°C)=920 J/Kg°C, Elongation= 9 %.

***7075 (Al-Zn-Mg) alloys* :** It is an alloy of Al with Zn as the main alloying element, it has a solidity comparable to many steels, has good resistance to fatigue and common machining, but has less corrosion resistance than many other Al alloys [16].

Table.2. 7075 alloy chemical composition.

Element	Si	Fe	Cu	Mn	Mg	Cr	Zn	Ti
Min % mass	-	-	1.2	-	2.1	0.18	5.1	-
Max % mass	0.4	0.5	2	0.3	2.9	0.28	6.1	0.2

The main additions to this alloy class are Zn and Mg. A preferential interaction between the large atoms of Mg and the small atoms of Zn gives particles improving the mechanical properties of the alloy, but they always remain extremely localized in corrosion leading to the creation of one or more small holes in the metal. The origin of this corrosion type is on the one hand in the lack of oxygen on a very reduced part. 7075 alloy has a high mechanical performance explaining its use among the main materials in aeronautical construction. Physical and mechanical properties of the Al 7075 alloy are described elsewhere [17]: ρ= 2.80 Kg/dm^3, Melting interval= 475-630 °C, Elasticity module= 72000 MPa, Thermal conductivity (0 at 100°C)= 130 W/M°C, Resistivity to 20°C= 5.2 µ'Ωcm, Elastic limit= 475 MPa, Limit at break R_m= 545 MPa, Mass thermal capacity (0 at 100°C)= 915 J/Kg°C, Elongation= 8 %. *Study context:* Advantages of using Al in the aeronautical sector: (Light weight, High resistance, Corrosion resistance). *Aerospace aluminum alloy*: 2XXX and 7XXX series are the two main series used in the manufacture of components for aviation. 2XXX series alloys are used in the manufacture of parts for the lower wing and the fuselage structure of the aircraft. 7XXX series alloys are used in components requiring greater strength, such as parts of the upper wing.

- Al 2024 can be used when high strength to weight ratios is required. Al 2024 T3 alloy has excellent fatigue resistance but low weldability. 2024 alloy is used in wing and fuselage structures due to the high stresses to which these components are subjected during its use.
- Al 7075 T6 has a resistance similar to that of many types of steel and good machinability and fatigue resistance properties, but low weldability due to its Zn content [18].

***Aluminum corrosion Types*:** there are several types (Uniform corrosion, Galvanic corrosion, Localized corrosion, Pitting corrosion, Intergranular corrosion, Stress corrosion) [9, 19, 20]. The interaction phenomena between the various parameters make it difficult to study the corrosion mechanism and determine the influence of each of these parameters. The mechanisms of intergranular corrosion, pitting corrosion or stress corrosion are widely described. Several points remain to be clarified, in particular the study in less aggressive environments which would allow not only to obtain an understanding of the passive film role in the sensitivity to corrosion of the two alloys, but also of that of intermetallic particles.

2. Experimental techniques

This part is dedicated to the experimental conditions and methods description implemented in this work for the corrosion behavior study of 2024-T4 and 7075-T6 aluminum alloys in aeronautical functional environments, thus their metallurgical states characterization.

2.1. Experimental protocols

2.1.1. Heat treatments parameter

It will be limited to a heat treatment by structural hardening in order to optimize the mechanical properties and corrosion resistance. In fact, it consists of three steps, we will start processing twelve samples for 2024 alloy and nine samples for 7075 alloy, so as to change each time only one parameter, that is the maintenance duration during dissolution or the annealing temperature or treatment without annealing. The heat treatments description applied to the two materials is given in the following table.

Table.3. Heat treatments description applied to the 2024 and 7075 alloy studied

Alloy	Steps	Dissolution		Temper	Returned	
	Treatment	T (°C)	Duration (mn)	Middle	T (°C)	Duration (mn)
2024	T0	-	-	-	-	-
	T1	495±5	15	Water	-	-
	T3	495±5	15	Water	-	-
	T4	495±5	15	Water	200±5	60
7075	T0	-	-	-	-	-
	T1	495±5	15	Water	-	-
	T2	540±5	60	Water	200	180

***Operating mode description**:*

We have assumed that the alloys are intended for an aeronautical application for which we will need to improve the mechanical properties of two alloys studied. The treatment to be carried out is a structural hardening heat treatment, for 2024 and 7075 alloys, at different temperatures and duration. The treatment quality in order to effectively demonstrate it depends on several parameters, namely: (oven nature, quench bath nature, maturation time, treatment duration, quenching duration, tempering temperature).

***Dissolution**:* After dissolution in an electric oven, we set the set point to the desired high temperature, we wait 40 minutes to arrive at this set point and then we introduce only four samples, placed on a metal support made in the forge workshop using the cutting process and a sheet bending. After maintaining these samples at (495°C, 15mn) in the oven, we take it out of the oven to water soc (13°C). In the same way we set the set point at the desired temperature and which is suitable for each type of treatment and alloys and for each treatment we take into account that four samples for 2024 alloy, and three samples for 7075 alloy.

Tempering and maturation:

The used tempering mode is immersion in water. In order to achieve significant results, the tempering must immediately follow the samples exit. It is for this reason that the metal support has been prepared to soak all the

samples at same time. Tempering was done in a bucket filled with water at 13°C. Directly after tempering, the samples were weighed; the samples were matured at room temperature and at five days.

***Returned**:* The samples, which have matured for five days, are kept at a temperature below that of dissolution, which depends on the alloy nature.

2.1.2. Microstructural state characterization

Sample mechanical preparation begins with cutting the sample, and good cutting will increase the quality of the sample final rendering. Once the cutting step has been performed, the second process step is coating the samples, the purpose of which is to be able to handle small irregularly shaped samples and protect the sharp edges in the polishing step Fig.1. In order to obtain a highly reflective surface, without scratching and deformation, the samples must be carefully rectified and polished with increasingly fine abrasive papers, and finalized by the diamond paste of alumina or silica, before they can be examined under an optical microscope.

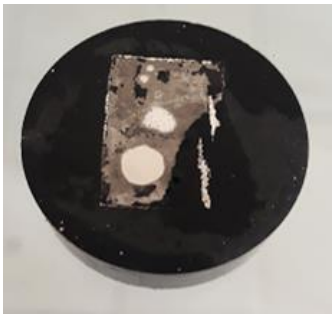

Fig.1. Coated sample before polishing

2.1.3. Vickers hardness test

Vickers method is a static hardness test method which is part of the standard methods (ISO 6507, ASTM E92, ASTM E384); it consists in applying a load P on the material for 10 to 15s with an indenter or indenter provided with a diamond point in the shape of a square pyramid with an apex angle between faces of 136°. In the Vickers hardness test, based on optical method, the impression size left by the indenter or the impression diagonal are measured using Toupview software. To have the very real and precise dimensions of the penetrations on the software, we made a calibration of 7cm → 100µm. To determine the Vickers hardness (HV) according to ISO 6507, the pyramidal indenter is pressed with a test load defined from gf against a coated sample. For the calculation of the remanent pyramidal footprint surface, the average value of the two diagonals d1 and d2 (mm) is used, the footprints base often not being exactly square. For the force used is 500gf = 4.9N, and the penetration time 15s.

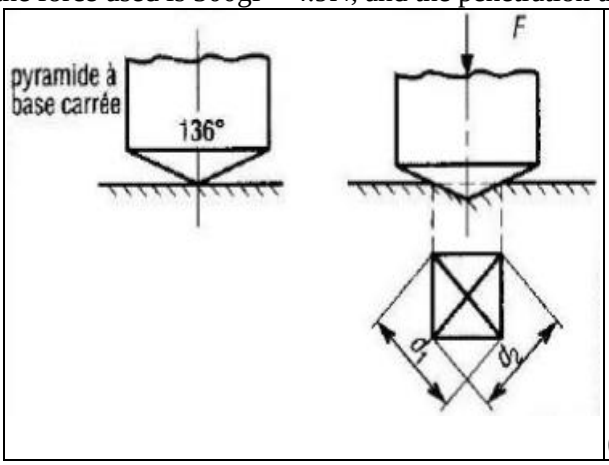

$$HV = 0.189\,\frac{F}{d^2}$$

avec

$$d = \frac{d_1 + d_2}{2}$$

$(F\ en\ N, d_1 et\ d_2\ en\ mm)$

Fig.2. Vickers test principle and conduct

2.2. Corrosion empirical study of 2024 and 7075 alloys

2.2.1. Corrosion tests normalization

So are corrosion test methods like unit systems; in order for corrosion tests results to be comparable from one laboratory to another, the need for common and normalized methods became very early evident, for example, that the first ASTM standard on salt spray testing goes back to the 1930s [3].

2.2.2. Salt spray test

The salt spray test, also called the salt spray test, which the machine is presented in figure 18, makes it possible to evaluate the corrosion resistance of metallic materials, whether with or without coating, temporary or permanent, of protection against corrosion. The conduct of these tests is described by different standards (ASTM B1171, DIN 500212, EN ISO 9227). In all cases, the parts to be evaluated are placed in a test chamber in which a saline solution is vaporized at a certain temperature. The test can be achieved continuously for six to over a thousand hours. The most corrosion resistant materials can be tested for longer. Salt spray essays are particularly useful for detecting discontinuities like pores or other defects of certain metallic coatings, anodic or of conversion layers.

***BS operating mode**:* According to ASTM B 117, we are based on eight treated samples of 2024 alloy and six treated samples of 7075 alloy. The samples did not require surface preparation; So, we put them directly into the BS machine, in a uniform way, allowing the test solution to reach the entire sample surface.

***Saline solution preparation**:*

Table.4. BS parameter of cycle N°1 and N°2

Cycle	Mode	Atmosphere	T (°C)	PH	Stay duration
N°1	NSS	Wet 5% of *NaCl* by mass	35	7	19h 40mn
N°2	NSS	Wet 5% of *NaCl* by mass	40	7	17h

According to ASTM D 1141, the saline solution was prepared using 5% by mass of sodium chloride in 95% of demineralized water. The pH of the solution was kept at its neutral position. The medium temperature was set at 35°C during cycle N°1 and 40°C during cycle N°2.

Positioning of the samples:

The position of the samples in the salt spray during the test must be such that the following conditions are met:

- Except otherwise indication, specimens were supported on a bench horizontal and parallel to the main direction of mist flow through the chamber, based on the dominant surface under test.
- The samples must never be in contact with each other or with any other metallic material or able body of acting as an aggressive element.
- Each specimen has to be placed in such a way as to allow the free flow of the mist over all the specimens.
- The salt solution of one sample must not touch the other samples.

2.2.3 Stress corrosion test

This type of corrosion can be assessed by a fairly wide range of configurations, and depending on the type of stress applied, the resistance to CSC is determined under different conditions. In this regard, we plan to evaluate the effect of

bending stress on the propagation of pits in the surface perpendicular to the sample surface. Based on the norm ASTM G47, we accomplished six samples of the alloy 7075 of a rectangular form of dimensions (57x10x2 mm^3). In effect, we were a product of a mechanical cleaning by abrasive paper of samples to assure a good preparation of surface, so we fixed them in a steel plate by varying the distance of ends with a solicitation in inflection of samples, while being sure that distortion remains elastic to study the influence of the module of inflection on corrosion under pressure. We then immersed the plate in a water bath assimilated to sea water, and the NaCl content of which is 5% by mass, for 15 days. Through this chapter, we were able to characterize the alloy studied during this project, as well as all the standards relating to the range of tests studied. Such an approach may introduce the reader in the context of evaluating the corrosion resistance of alloy 2024 by comparing it with alloy 7075, given that they are both under the same conditions in aeronautics.

3. Results and discussions

This part includes the results discussion from all the corrosion tests for the 2024 and 7075 alloys treated. While being based on scientific interpretations (analytical, numerical, and empirical), this discussion offers a modest contribution towards a better understanding of the phenomena responsible for the behavior of 2024 and 7075 alloys towards corrosion.

3.1. Microstructural characterization

The micrographic observation under optical microscope of the samples, having undergone heat treatments revealed the microstructures represented below:

***2024 alloy*:**

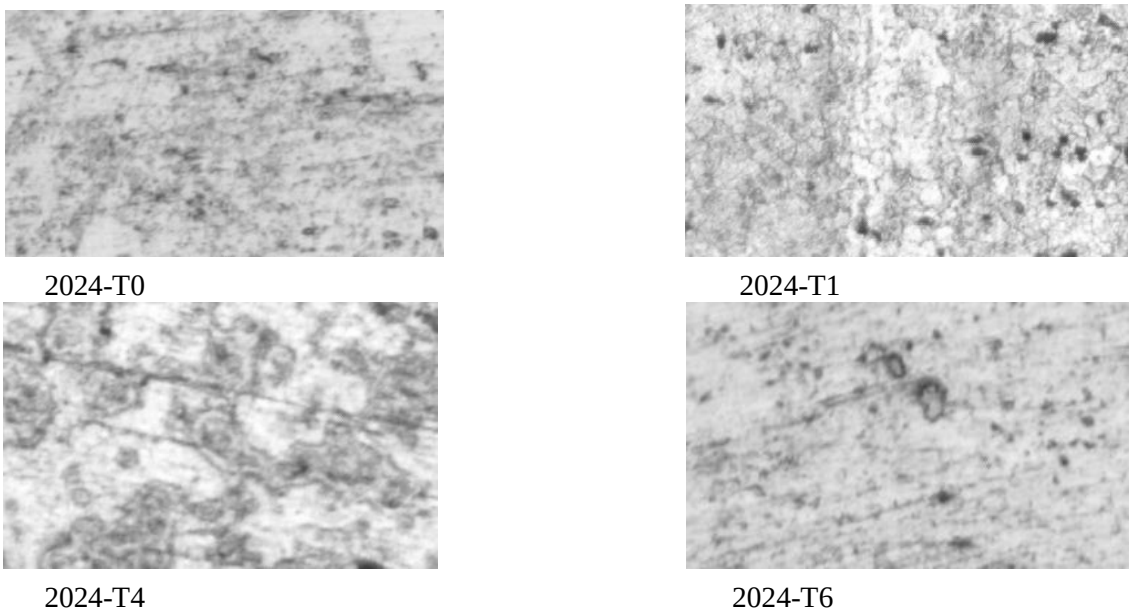

2024-T0 2024-T1

2024-T4 2024-T6

Fig.3. Micrographic observation under optical microscope of 2024 alloy.

- The 2024-T0 sample has only one phase with a high puncture rate compared to the other samples.
- The 2024-T1 sample has undergone a dissolution and a rapid quench, marks the presence of a phase rich in aluminum and other rich in precipitates Al_2Cu.
- The 2024-T4 sample, we clearly notice the presence of two phases, one dark rich in copper and Al_2Cu, and the other clear rich in aluminum.

- The 2024-T6 sample, has undergone a tempering at a temperature of 200°C for one hour, has two phases, one rich in aluminum and the other rich in Al_2Cu precipitates.
- The 7075-T0 sample shows the different chemical compounds of the alloy, Aluminum, Zinc and Magnesium, as well as the surface degradation.
- The 7075-T1 sample underwent a solution treatment and quenching, shows the precipitates formed during tempering $MnZn_2$ and a non-high bite rate seen quenching.
- The 7075-T6 sample has tempered after quenching, clearly shows the chemical stability of the alloy and no longer shows a surface degradation than other samples 7075-T0 and 7075-T1.

- ***7075 alloy:***

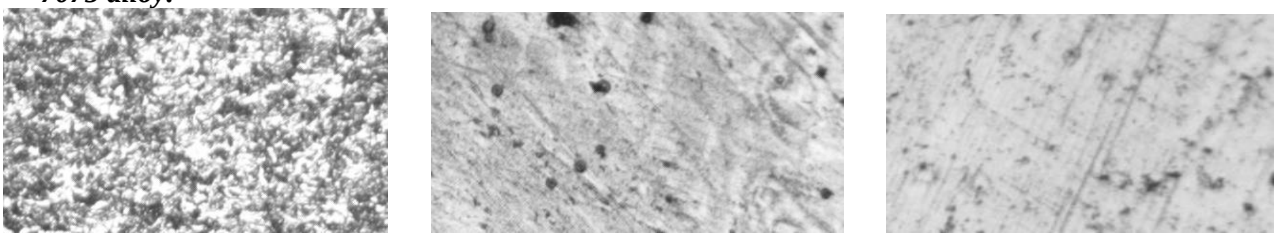

7075-T0 7075-T1 7075-T6

Fig.4. Micrographic observation under optical microscope of 7075 alloy.

3.2. Hardness analysis

Each of the samples has undergone a different heat treatment, the hardness of five penetrations for each sample is calculated. From table.5, it is found that the control samples of the two alloys 2024 and 7075 have the minimum hardness values compared to the others which have undergone the heat treatments. However, the samples having undergone a T6 treatment have the maximum hardness values. To be able to make effective and correct interpretations, it was first necessary to seek the connection between hardness and heat treatments.

Table.5. HV hardness measurements for 2024 and 7075 alloys

	Witness (T0)	Hardened (T1)	Matured (T4)	Returned (T6)
Hardness (HV) (2024 alloys)	35.46	41.56	85.44	95.56
Hardness (HV) (7075 alloys)	25.89	95.20	---	104.48

For 2024 alloy :

During the structural hardening treatment, the hardening precipitates (Al_2Cu) are formed, which translates the improvement in the mechanical properties and then in the important hardness values for T4 and T6 samples. Furthermore, the T1 treatment (dissolving and quenching) must in reality have a softening then lower hardness values which therefore contradict our case study, because the soaked samples continued their treatment for a week at free air and therefore natural aging known as maturation, the thing that makes it possible to obtain higher hardness values.

For 7075 alloy:

Like the 2024-T1 alloy, the 7075 alloy exhibited respectable hardness values because it was matured in the open air. And for 7075-T6 alloy, in turn presents higher hardness values.

2024-T4 et 7075-T6 :

As recently mentioned, we take into account that the alloys used in the aeronautical sector, that is to say the 2024-T4 and 7075-T6 alloys. The microhardness of 7075-T6 is greater than that of 2024-T4 due to the Mg and Zn precipitates formed during the heat treatment, while in 2024-T3 the Cu and Mg precipitates are less important in hardness terms.

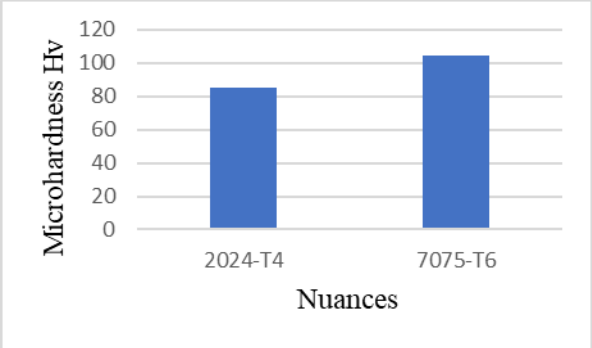

Fig.5. Alloys vickers microhardness

3.3. Assessment of uniform corrosion resistance

The mass loss is a fairly important indicator for our preliminary study of the uniform corrosion aspects, so we measured the samples mass of each alloy and later calculated the mass loss. Like any other relative deviation, the mass loss is calculated by the difference in mass compared to the sample mass before the BS test; it is expressed by the following formula:

$$Mass\ loss = \frac{\Delta m}{m_0} = \frac{m_f - m_i}{m_i}$$

**** For the 2024 alloy at 35°C :***

The following tables present the masses before and after the BS test, with residence time is 19h 40mn : From these results, we note that (1) and (2) samples have the same evolutionary trend, which allowed us to take into account only (1) sample of each treatment.

Table.6. Masses before and after the BS test

Echantillon		m_i (g)	m_f (g)
Witness T0	1	2.014	2.022
	2	3.004	3.013
Tempered T1	1	2.013	2.020
	2	2.999	3.010
Matured T4	1	2.015	2.020
	2	3.003	3.013
Revenue T6	1	2.014	2.022
	2	2.995	3.022

The following figure shows the mass loss as a function of time in BS test at 35 °C. From Fig.6, we can clearly see that in the first hours of the BS test, the curve indicates a mass gain and no longer a mass loss. Indeed, empirically, the need to have a mass loss is linked to the surface degradation phenomenon under the corrosive medium effect, while in our case, the degradation mechanism in the solid-liquid interface is counterbalanced by the hydroxyl salts effect which result from the alloy oxidation, as well as the deposition and interaction of mineral salts with the alloy surface.

o Between points 1 (3h) and 2 (5h10mn) the first peak of the curve at 5h, 10mn indicates the passivating layer rupture in contact with the aggressive medium which is sprayed saline water, and the T0, T1 and T4 samples have significant mass gain values.

o Between points 2 (5h 10mn) and 3 (11h 40mn) the mass gain is less important because it is compensated by the passivating layer formation of chemical formula Al_2O_3 which forms spontaneously in the oxidizing medium.

Between points 3 (11h 40mn) and 8 (20h) the 2024-T4 sample begins its passivation process and therefore displays a better corrosion resistance compared to the 2024-T1 and 2024-T6 samples.

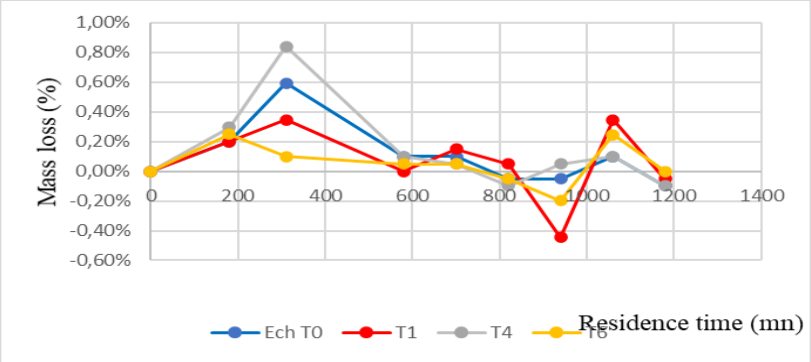

Fig.6. Mass evolution in salt spray at 35 °C

For the 2024 alloy at 40°C:

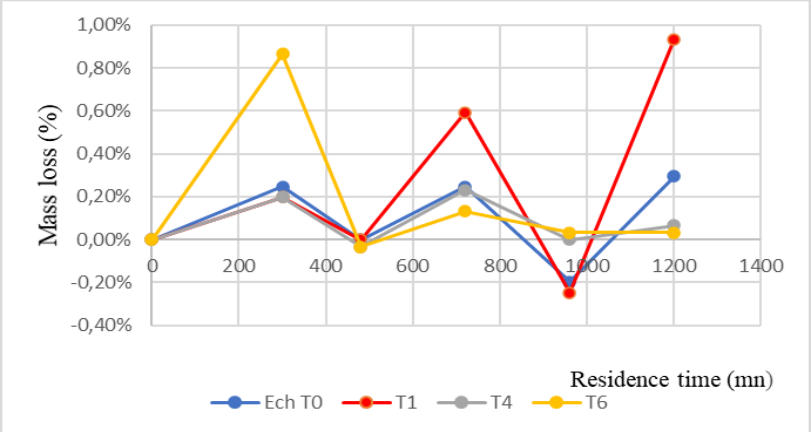

Fig.7. Mass evolution in salt spray at 40 ° C

o The mass gain of the control sample is practically invariable between point 1 (3h) and point 3 (12h) as well for T4 sample.

o The T6 sample shows a mass gain in point 1 (3h) due to the salt mass and aluminum hydroxide $Al(OH)_3$.

o The T6 and T4 samples between point 4 (16h) and 5 (20h) show better values compared to T0 sample, and therefore T4 and T6 samples are more resistant to uniform corrosion than T0 and T1 sample.

For 7075 alloy at 35 °C:

Following tables present the masses before and after the BS test, with residence time is 19h 40mn: Considering that of a sample for each treatment, the following figure present the mass loss of 7075 alloy at 35 °C as a function of time: From Fig.8, we note that all the samples of 7075 alloy have followed a mass gain followed by a mass loss during the whole residence time. Furthermore, the mass loss values for the T6 sample show its best corrosion resistance until the stay end.

Table.7. Masses before and after the BS test.

Sample		m_i (g)	m_f (g)
Witness T0	1	2.256	2.260
	2	2.511	2.518
Tempered T1	1	2.907	2.911
	2	2.487	2.492
Revenue T6	1	2.625	2.633
	2	2.319	2.331

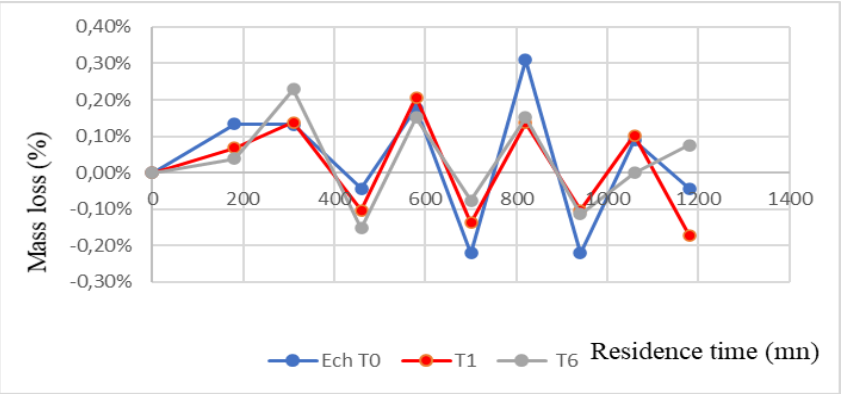

Fig.8. Mass loss in salt spray at 35 °C

7075 alloy at 40°C :

For the T0 (control) sample and T1 followed a mass degradation during the stay first hours, on the contrary the T6 sample presented mass gain values not significant which shows their chemical stability thus its best corrosion resistance.

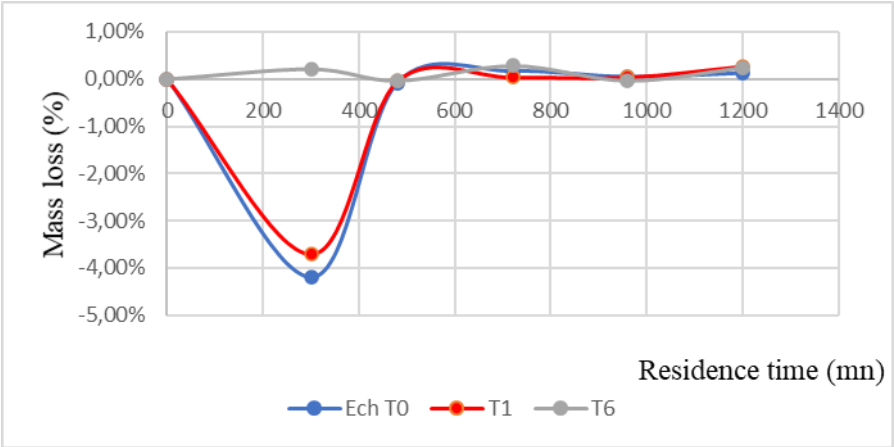

Fig.9. Mass loss in salt spray at 40 °C

3.4. Resistance evaluation to corrosion by pitting

Contrary to uniform corrosion, the intensity and rate of corrosion by pitting cannot be evaluated neither by weight change neither by hydrogen released measurement. These measures do not make sense, because a very deep and isolated bite results in a small decrease in weight, while very many superficial bites can cause a very strong decrease in weight. Density measurement presents no particular difficulty, since it suffices to count the visible pits number on a surface or on a representative length. Experience shows that the square decimetre if it is a sheet, and the decimetre if it

is a tube, are very sufficient to get a good indication of the density. Using a standard charter of ASTM G 46, the evolution of the pitting density for the 2024-T4 and 7075-T6 alloys for the samples from BS is evaluated.

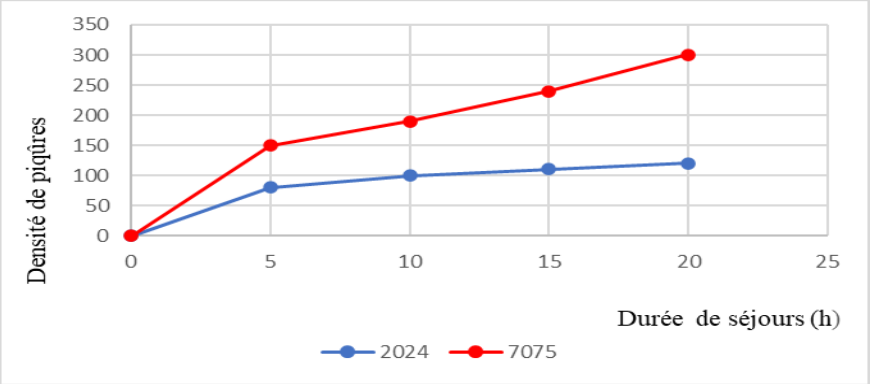

Fig.10. Pitting density as a function of alloys

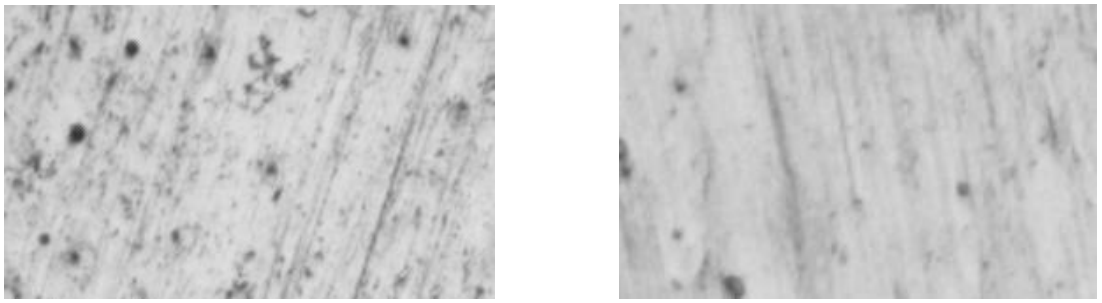

7075-T6 2024-T4

Fig.11. Puncture density under optical microscope for the alloys after attack by Keller solution for 15s.

The obtained results from these micrographs validate the curves mentioned in Fig.11. A descriptive analysis of the bites dispersion on the samples surfaces clearly indicates that the 7075-T6 alloy is more sensitive to pitting than the 2024-T4 alloy under the BS test conditions. This observation always remains true for temperatures below 250°C [21]; while starting from this thermal threshold, the samples surfaces evoke a distinguished behavior for which the 7075-T6 alloy surface repassivates by forming an oxide layer chemically stable with respect to neutral oxidizing media (Absence sulfur compounds); this limits the new bites formation at the alloy surface. On the other hand, in the case of our alloy (2024-T4), the repassivation kinetics at high temperature (T>250°C) is limited, which increases the pitting probability on the alloy surface.

3.5. Resistance assessment of to stress corrosion

As indicated before, the choice of bending stress is attributed to conditions comparable to those of the aeronautical environment, except for error. The starting point before performing any analysis type is to calculate the stresses applied to the studied samples.

$$L = \left(\frac{ktE}{\sigma}\right) Sin^{-1}\left(\frac{H\sigma}{ktE}\right)$$

L: Specimen length; H: Distance between supports; T: Specimen thickness; σ: Applied fatigue stress.

$K = \int_0^{\frac{\pi}{2}} (1 - k^2 sin^2 z)^{-1/2} dz$; Complete elliptical integral of the first type

$E = \int_0^{\frac{\pi}{2}} (1 - k^2 sin^2 z)^{1/2} dz$; Complete elliptical integral of the second type

$k = \sin(\theta/2)$

θ: Maximum angle at the end of the specimen; and z: Integration parameter

Thus, the applied stress calculation will begin by determining the problem parameters which are explained above:

$$\frac{\sigma}{sin^{-1}(b\sigma)} - a = 0 \;; \quad a = \frac{ktE}{L} \;; \quad b = \frac{H}{La}$$

And the flexural deformation can be calculated directly from the following equation:

$$\sigma = 4(2E - K)\left[\frac{k}{2} - \frac{2E - K}{12}\left(\frac{t}{H}\right)\right]\frac{t}{H}$$

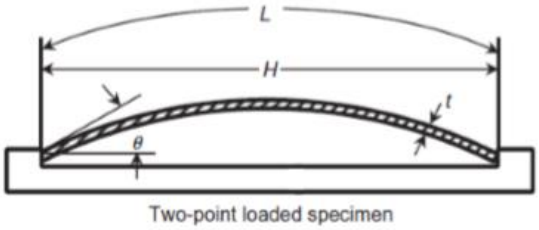

Fig.12. CSC assembly configuration for 7075-T6 sample.

All of these calculations can only be addressed after the calculations of variables mentioned above. In the same way as in the Salt Spray, the sensitivity of the 7075-T6 alloy to pitting is evaluated, by optical micrographic. The following figure shows the microstructural evolution of the bite density of the 7075-T6 alloy samples after 15 days of immersion in saline water for a magnification of 100 after attack by Keller solution for 10s. By observing these microstructures, the reader can note that the pitting density of the 7075-T6 alloy after the test (on the left) is much higher than that observed before the test (on the right). So we can conclude that in bending mode, and in a salt water bath the alloy 7075-T6 is very sensitive to pitting. To be more precise, and to validate their pitting sensitivity, we take into account the stress effect applied on the pitting propagation at the samples surface. In Fig.21, we indicate the results noticed in terms of the bite surface evolution; the 4 adjacent micrographs represent the sample from the most flexed area of each assembly, which of course corresponds to the most unfavorable case.

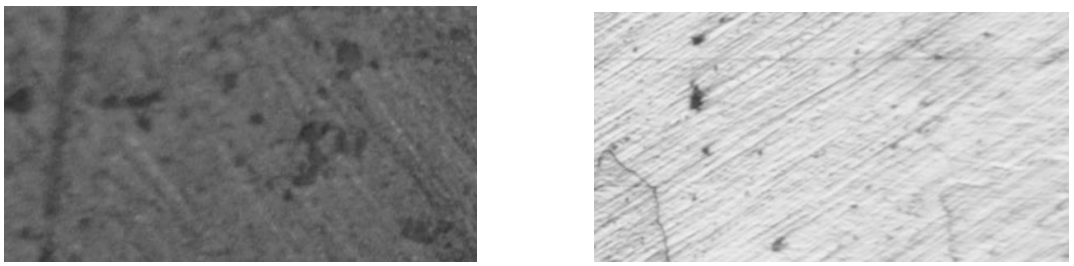

Fig.13. Bite density microstructural evolution of 7075-T6 alloy samples.

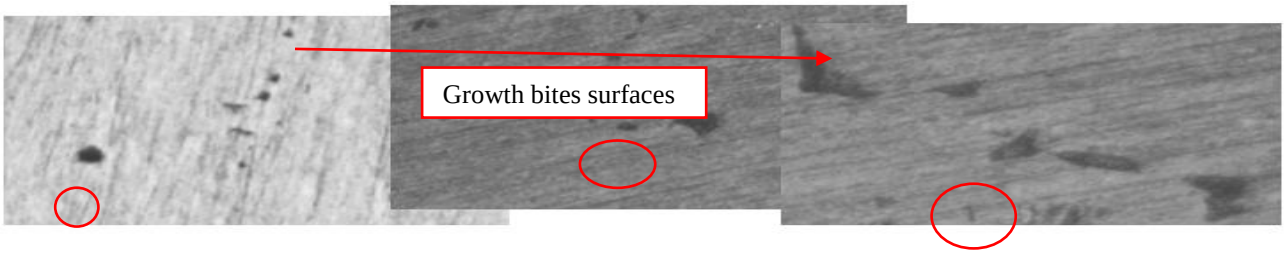

Fig.14. Bite surface evolution as a function of maximum stress applied for 7075-T6 alloy with 100 magnification.

It is very clear, after the evolution analysis of pitting surface that the 7075-T6 alloy is very sensitive to pitting corrosion under the parameters effect of bending stresses as well as the salt water bath. The tests range allowed us to characterize the corrosion resistance of 2024-T4 and 7075-T6 alloys under the same conditions, while being based on the quantitative evaluation of several corrosion performance indices (mass loss, microstructural appearance, microhardness, bite density, and bite surface).

Conclusion

The main purpose of the work presented in this project is to characterize the behaviors of the most used 2024-T4 and 7075-T6 alloys in the contemporary aeronautical field, and to determine the effect of heat treatments on them. To do this, it was necessary to perform a set of standardized tests, based on ASTM standards and the ISO organization, in order to follow the evolution of the microstructure by optical microscope and Vickers hardness as well to see their corrosion behavior in corrosive environments in the BS and CSC tests. In terms of the study's prospects, our studies during this work allowed us to make a modest contribution, but rigorous to the scientific world of evaluating the corrosion resistance of 2024-T4 and 7075-T6 aluminum alloys. However, this study may be preliminary in thinking of solutions or remedies against corrosion, such as:

- Chromate coatings, recognized as toxic, for aeronautical alloys and why not protective coatings, therefore toxic, replacing chromate.
- Sol-gel bio-coatings for anticorrosion.

Reference

[1] Gupta VK, Agnew SR, *Int. J. Fatigue*, 33(9) (2011) 1159-1174.

[2] Andreatta F, Terryn H, de Wit JHW, *Electrochimica Acta*., 49(17-18) (2004) 2851-2862.

[3] a) C. Vargel, *Corrosion of Aluminium*, 1st ed. Paris: Elsevier; (2004) 601 p.
b) A. Ziouche, A. Hammouda, N. Boucherou, M. Mokhtari, B. Hafez, H. Elmsellem, S. Abaidia, *Mor. J. Chem*. 9 N°3 (2021) 386-393.

[4] Henry Sainte-Claire Deville, *Revue de l'aluminium*, 211 (1954) 97.

[5] K. Mizuno, A. Nylund, I. Olefjord, *Corros. Sci.*, 43 (2001) 381-396.

[6] M. Mokaddem, J. Tardelli, K. Ogle, E. Rocca, P. Volovitch, *Electrochem. Commun.* 13 (1) (2011) 42-45.

[7] S. Lebouil, J. Tardelli, E. Rocca, P. Volovitch, K. Ogle, *Mater. Corros.*, 65 (2014) 416-424.

[8] P. Volovitch, M. Serdechnova, K. Ogle, *Corrosion.*, 68 (2012) 557-570.

[9] C. Sorriano, R. Oltra, A. Zimmer, B. Vuillemin, C. Borkowski, *Surf. Interface. Anal.*, 45(10) (2013) 1649-1653.

[10] S.C. Wang, M.J. Starink, N. Gao., *Scripta Materialia*, 54 (2006) 287-291.

[11] M. Asano, T. Minoda, Y. Ozeki H. Yoshida, 10th ICAA, *Mater. Sci. Forum*, (2006) 771-776.

[12] Peter C. King, Ivan S. Cole, Penny A. Corrigan, Anthony E. Hughes, Tim H. Muster, *Corros. Sci.*, 53, (2011) 1086-1096.

[13] Handbook ASM, E. H. Hollingsworth, H. Y. Hunsicker, *Handbook. ASM*, 30 (1990) 583-609.

[14] D. G. Eskin, L. Katgerman, Suyitno, J. F. Mooney, *Metall. Mater. Trans A*, 35 (2004) 1325-1335.

[15] Cevdet Meric, *Mater. Res. Bull.*, 35 (2000) 1479-1494.

[16] a) O. Hatamlet, M. Preet, J. Singh, H. Garmestani, *Corros. Sci*., 51 (2008) 135-143.
b) L. C. L. A. Jamshidi, R. J. Rodbari, L. Nascimento, E. P. Hernandez, C. M. B. M. Barbosa, *Mor. J. Chem*. 6 N°3(2018) 445-454.

[17] Gokhan Ozer, Ahmet Karaaslan, *Trans. Nonferrous Met. Soc. China*, 27 (2017) 2357-2362.

[18] Lourenço JC, Faria MIST, Robin A, Prisco LP, Puccini MC, *Mater. Corros.*, 66(12) (2015) 1498-1503.

[19] M. Reboul, Corrosion des alliages d'aluminium (COR325), *Techniques de l'ingénieur*, 06 (2005) 1-18.

[20] A. M. Ayuba, A. Uzairu, H. Abba, G. A. Shallangwa, *Mor. J. Chem*. 6 N°1 (2018) 160-172.

[21] Pang JJ, Liu FC, Liu J, Tan MJ, Blackwood DJ, *Corros. Sci.*, 106 (2016) 217-228.